J. Fluid Mech. (1982), *vol.* 115, *pp.* 453-474
Printed in Great Britain

An experimental study of small-amplitude drop oscillations in immiscible liquid systems

By E. TRINH, A. ZWERN AND T. G. WANG
Jet Propulsion Laboratory, California Institute of Technology, Pasadena

(Received 9 January 1981 and in revised form 25 June 1981)

Measurements of the characteristics of small-amplitude shape oscillations of drops immersed in a host liquid have been carried out by acoustical means. The resonance frequencies of the first few modes have been measured, as well as the damping constant for the fundamental mode, as functions of the drop radius and viscosities of the two liquids. A qualitative photographic study during steady oscillations has revealed a simple internal fluid-particle flow field with no circulation. The theory available at the present time has been found to provide results which are in general agreement with experimental findings for low-viscosity liquids.

1. Introduction

The dynamics of free liquid drops has long been a subject of interest (Wang, Saffren & Elleman 1974), both for the sake of basic scientific understanding as well as for various applications in meteorology and chemical industry. The rigorous treatment of the problem of liquid drops oscillating in a gravitational field is complicated by the fact that, for most droplets of practical size, surface-tension forces and gravity are two competing factors influencing the dynamics of such oscillations. This is the limitation inherent to all laboratory work. Experiments carried out in the low gravity of space flight may not suffer from such interference, but other complications arise from the remote operations (Wang 1979; Jacobi *et al.* 1979). In immiscible liquid systems, the effects of gravity can be made negligible, although other difficulties arise owing to the mass loading from the outer host liquid, from boundary layer dissipation, as well as from the external field used to excite the drop oscillations. Both theoretical and experimental treatments of liquid-drop oscillations have appeared in the literature (Miller & Scriven 1968; Marston & Apfel 1980) although they have been restricted to the limiting case of small-amplitude vibrations. In this paper we would like to report on the first part of our detailed study of drop-shape oscillations in immiscible liquid systems. Here, we shall confine our attention to small-amplitude vibrations (i.e. $\Delta D/D < 0{\cdot}1$), while a companion report (Trinh & Wang 1980) describes our results in the large-amplitude region (i.e. $\Delta D/D > 0{\cdot}1$). Such a separation of the subject matter only reflects the fact that the phenomena we observed in the large-amplitude region could no longer be described by the existing linear theory. It should be noted, however, that there is no arbitrary threshold for the value of the oscillation amplitude above which nonlinear effects are observed.

In this particular paper, we shall be interested in the measurement of the first few resonance frequencies and the damping constant in the small-amplitude region as

both the drop size and the viscosity are varied. Viscosities varying between 1·3 and 130 cSt will be studied, and the drop diameter will range between 0·5 and 1·5 cm. The experimental method involves acoustic levitation and radiation-pressure-force modulation (Marston & Apfel 1979). In addition to quantitative information about the various resonance modes of the drop, a qualitative treatment of the characteristics of the internal fluid particle flow field has also been obtained. Comparison with available theoretical predictions was generally favourable when appropriate precautions had been taken to satisfy the theoretical assumptions. It then appears, at least for the steady-state or long-time behaviour, that the linear theory yields satisfactory answers to the problem at hand. No detailed study of a possible transient regime has been carried out in this work.

We shall first undertake a short summary of the published theoretical results. We then describe the experimental apparatus and methods will then follow. A discussion of the experimental results and a comparison with the theory will close the paper.

As a final general remark, we would like to point out that the present experimental technique minimizes the external effects upon the drop's behaviour; such interference cannot, however, be totally eliminated. An absolutely rigorous comparison with theoretical claims cannot be obtained, although we feel that at least for small-amplitude oscillations we are fairly close.

2. Theoretical background

Miller & Scriven (1968) have provided a rather comprehensive theoretical analysis of the natural, small-amplitude, shape oscillations of a drop by using the normal-mode framework. Marston (1980) has offered an independent derivation for the case of a liquid drop immersed in a fluid of similar properties, adding a small correction term to the damping constant. Prosperetti (1980) has obtained a solution to the initial-value problem, and has provided theoretical predictions concerning the behaviour of a freely oscillating drop in the early transient period.

An expression for the Lth resonant mode frequency of a driven oscillating drop is given by

$$\omega_L = \omega_L^* - \tfrac{1}{2}\alpha\omega^{*\frac{1}{2}} + \tfrac{1}{4}\alpha^2, \tag{1}$$

where ω_L is the angular response frequency, and ω_L^* is Lamb's natural resonance frequency (Lamb 1932) expressed as

$$(\omega_L^*)^2 = \frac{L(L+1)(L-1)(L+2)}{R^3[L\rho_o + (L+1)\rho_i]}\sigma. \tag{2}$$

R is the radius of the undisturbed drop, σ is the interfacial tension, and ρ_i and ρ_o the density of the inner and outer liquid respectively. α is given by

$$\alpha = \frac{(2L+1)^2(\mu_i\mu_o\rho_i\rho_o)^{\frac{1}{2}}}{2^{\frac{1}{2}}R[L\rho_o + (L+1)\rho_i][(\mu_i\rho_i)^{\frac{1}{2}} + (\mu_o\rho_o)^{\frac{1}{2}}]}, \tag{3}$$

μ_i and μ_o being the dynamic viscosity of the two liquids.

The free decay of an oscillating drop is characterized by the damping constant τ_L^{-1}, expressed as

$$\tau_L^{-1} = \tfrac{1}{2}\alpha\omega_L^{*\frac{1}{2}} + \tfrac{1}{2}\gamma - \tfrac{1}{2}\alpha^2, \tag{4}$$

where

$$\gamma = \frac{(2L+1)\{2(L^2-1)\mu_i^2\rho_i + 2L(L+1)\mu_o^2\rho_o + \mu_i\mu_o[(L+2)\rho_i - (L-1)\rho_o]\}}{R^2[(\mu_i\rho_i)^{\frac{1}{2}} + (\mu_o\rho_o)^{\frac{1}{2}}]^2[L\rho_o + (L+1)\rho_i]}. \quad (5)$$

One might notice that the expression for the damping constant τ_L^{-1} contains a term proportional to the square root of the natural resonance frequency. This term has been attributed to the dissipation arising in the boundary layer around the drop. The second term in (4) is associated with viscous dissipation within the bulk of the liquids, and is equivalent to the damping normally associated with the well-known damped harmonic oscillator.

The results presented here are valid when the assumptions of small-amplitude oscillations, vanishing tangential stress sources at the drop boundary, freedom from contamination, and the absence of internal circulation within the drop are satisfied. No dependence upon the oscillation amplitude for the resonance frequency or damping constant can be arrived at, and the various resonance modes are assumed to be uncoupled. One might also note that each mode of oscillation denoted by an integer L is actually degenerate. For example, in the fundamental-mode case where $L = 2$, there are five degenerate modes (corresponding to the integers $m = \pm 2, \pm 1, 0$) having the same frequency, but which differ in their geometry of oscillation. In this work we shall restrict ourselves to the axisymmetric mode ($m = 0$). The axis of symmetry will be that of the acoustic field, as will be shown below.

3. Experimental background

Generalities

A liquid drop can be trapped at a stable position in an acoustic standing wave existing in a resonant cavity filled with liquid. The static equilibrium shape of the drop can be controlled by varying the magnitude of the acoustic radiation force, which is, to second order, proportional to the square of the magnitude of the first-order acoustic pressure. In this case the cavity is of rectangular geometry, and the axis of symmetry is taken as its vertical axis. Depending upon the standing acoustic wave, or the pressure intensity, a drop may be given the shape of a prolate spheroid, an oblate spheroid, or a nearly perfect sphere.

Shape oscillations are induced through a low-frequency modulation of the acoustic radiation force. The excitation can be that corresponding to either a periodic elongation of the drop at the poles, or a periodic compression of the drop at the poles. The restoring force is, in the ideal case, provided only by the interfacial tension which tends to drive the drop back to the equilibrium shape. For low-amplitude vibrations both modes will yield the same results for the resonance frequency, although this shall not be the case for large displacements (Trinh & Wang 1980).

Various liquids have been used for both drop and host media. First the combination of a phenetole drop suspended in a 1:2 by volume mixture of methanol and distilled water was used. Next, various viscosity grades of Dow Corning silicone oil (5–200 cSt) were mixed with carbon tetrachloride to form drops which were suspended in distilled water. All drop liquids were coloured with oil-soluble dyes.

The acoustic frequencies were either 22 kHz ($\lambda \simeq 6{\cdot}75$ cm in water) or 66 kHz ($\lambda \simeq 2{\cdot}25$ cm in water). For a water host the kR parameter had values between 0·23

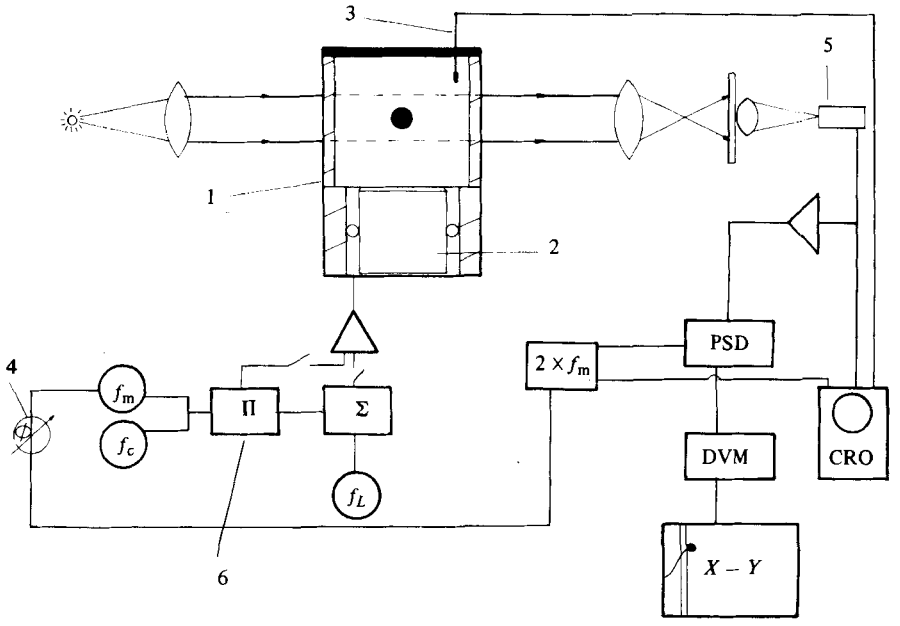

FIGURE 1. The experimental apparatus. 1 is the Lucite acoustic cell, 2 is the piezoelectric transducer, 3 is a hydrophone, 4 is a variable phase shifter, 5 is a photodetector, 6 is a balanced modulator. The $2 \times f_m$ frequency doubler supplies a reference signal with a determined phase relationship with respect to the hydrophone signal.

and 0·69 at 22 kHz, and between 0·69 and 2·1 at 66 kHz. Here k denotes the magnitude of the acoustic wave vector $(2\pi/\lambda)$ and R is the radius of the drop.

The drop oscillation amplitude is monitored using an optical detection technique: a slit parallel or perpendicular to the axis of symmetry is uniformly illuminated, the shadow of the drop is then centred across the slit, blocking some of the light. As the drop oscillates, the light intensity detected by a photo-transistor varies periodically in phase. Up to reasonably large amplitude the response has been found to be approximately proportional to the drop deformation. If the drop axis rotates, however, the detector will no longer yield a true maximum amplitude variation.

The apparatus and method

The hardware. A schematic representation of the experimental apparatus is given by figure 1. The acoustic cavity is made from a Lucite rectangular box with flat parallel walls (1). A hollow piezoelectric cylinder (2) with an aluminium plate glued with epoxy resin to one end provides a bottom to the box. The top of the cavity is a flat and rigid reflecting plate. The transducer can be driven in its fundamental longitudinal resonance (approx. 22 kHz), or at its third harmonic (approx. 66 kHz). The height of the resonant cavity may be adjusted by changing the liquid path, but the cross-section remains fixed. At 22 kHz and a cavity height of 11·5 cm, the acoustic pressure field has three equally spaced pressure maxima along the vertical central axis of symmetry. In any particular plane perpendicular to this axis, the pressure is a monotonically decreasing function of the distance from the centre. With this particular pressure distribution, a drop having a higher compressibility than the host liquid will

find a stable equilibrium position near the acoustic pressure maxima. A theoretical analysis of the translational force of acoustic radiation pressure in an immiscible liquid system has been provided by Yosioka & Kawasima (1955).

In order to drive the drop into oscillations, the acoustic pressure intensity is time-modulated at low frequency by superimposing two pressure waves of slightly different frequencies at the drop position. The difference frequency (denoted by $2f_m$) will be the acoustic-force modulation frequency. This was realized in practice with a balanced modulator multiplying a high-frequency carrier wave ($f_c = 22$ kHz or 66 kHz) by a low-frequency signal f_m. The two resonant frequencies of the cavity (22 or 66 kHz) may be used for either levitation or oscillation. For example, the simplest situation would involve only a 22 kHz signal multiplied by a low-frequency wave. This combination would achieve both stable levitation and drop-shape oscillation for a sufficiently small value of the density mismatch. One might also use a 66 kHz signal instead of the 22 kHz wave. In general, the first combination would provide a drive where the drop is compressed at the poles, and the second combination an elongation of the drop at the poles.

Data-analysis methods. The signal from the photodetector can either be analyzed directly on the oscilloscope, or through a lock-in amplifier (PSD on figure 1) for the extraction of more precise phase information. A reference wave at the force modulation frequency is provided by a frequency doubler ($2f_m$ on figure 1). An oscilloscope trace of such a reference signal is shown in figure 2, together with the output of a pressure hydrophone placed in the liquid cavity and driven by a 22 kHz signal multiplied by a 4 Hz wave. This particular picture describes a reference wave where the peak positive displacement is shifted by $+90°$ with respect to the peak of the acoustic pressure swing. The acoustic pressure squared, i.e. $P_r \propto \langle (P_{ac})^2 \rangle$. The time average in this case is performed over the period of the high-frequency carrier wave f_c^{-1}. If the acoustic pressure is given by

$$P_{ac} \propto \cos \omega_m t \cos \omega_c t, \tag{6}$$

then the force is

$$P_r \propto \cos^2 \omega_m t. \tag{7}$$

The positive peaks for P_r should be in phase with those of P_{ac}. The time variation and phase relationship of the radiation-pressure force and the reference wave should then be like those depicted in figure 3. A photodetector output in phase with this reference signal should then be that of a drop response in phase quadrature with the driving force.

One should note that the time average over f_m^{-1} does not yield a zero radiation-pressure force, i.e.

$$\langle P_r \rangle \propto \langle \cos^2 \omega_m t \rangle = \langle \tfrac{1}{2}(1 + \cos 2\omega_m t) \rangle. \tag{8}$$

There remains a steady-state force acting on the drop, together with a slow time-varying driving force. This steady force, if large enough, will deform the drop into a non-spherical equilibrium shape. For low-amplitude oscillations such distortion will

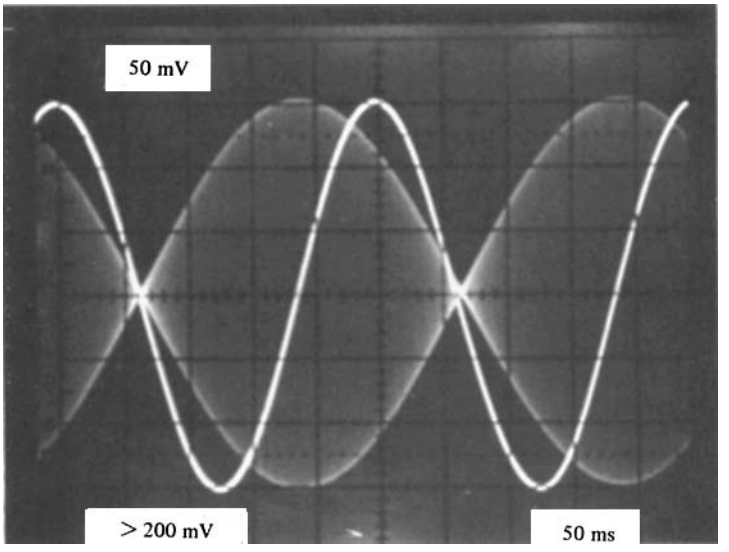

FIGURE 2. Oscilloscope traces of hydrophone output (envelope), and reference signal. Here the reference signal peak is shifted by $+90°$ with respect to the peak of the hydrophone output signal.

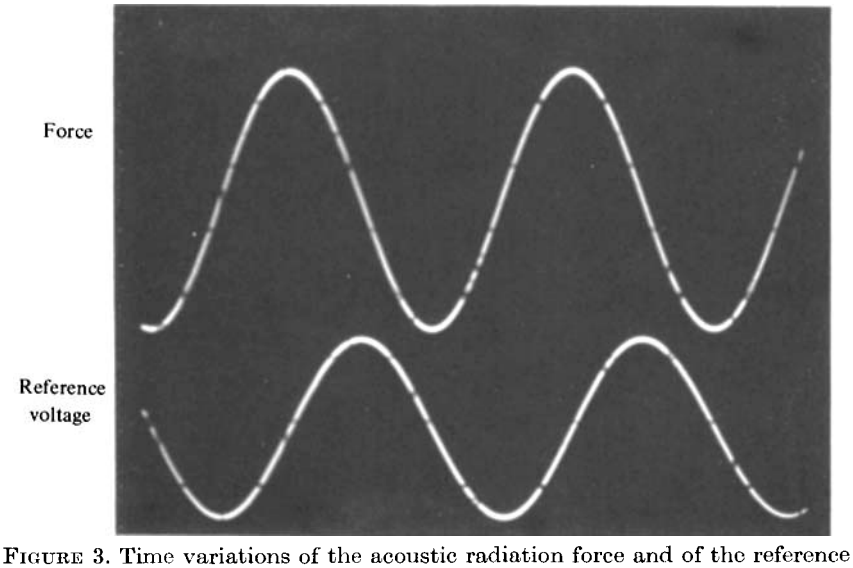

FIGURE 3. Time variations of the acoustic radiation force and of the reference wave. The latter wave is phase-shifted by $+90°$.

be small (less than 1 % deviation from the spherical shape), but it will become significant when large-amplitude oscillations are considered.

Steady-state measurements can be obtained together with swept-frequency responses. A slow linear sweep for the modulation frequency f_m allows the determination of the resonance frequency spectrum. Care must be taken to sweep very slowly in order to obtain the true amplitude resonance curve.

The phase of the drop response to steady-state excitation is measured by a lock-in

amplifier as a function of frequency. The damping constant for the fundamental mode may be obtained through such a measurement (Marston & Apfel 1980). In general, however, our decay constant results have been gathered through direct measurements on photographs of oscilloscope traces obtained during free decay. A faster but less accurate method would be to measure the width of the resonance curve.

Steady equilibrium shapes of drops were determined through magnified still photographs. The dynamics of the oscillations were also analysed through high-speed ciné films.

4. Resonance frequencies

Fundamental axisymmetric mode ($L = 2$, $m = 0$)

Generalities. The resonance frequency of the fundamental mode has been measured as a function of size and for various liquids. In all cases the density mismatch between the drop and host liquids was less than 1 %.

When measuring the resonance frequency by maximizing the quadrature response, the precision can be as high as 1 part in 2000. The repeatability of such a measurement on different drops, however, is strongly affected by the high sensitivity of the interfacial tension to the variations in the level of contaminants found in both the drop and host liquids. Two observed phenomena might be the symptoms of such a contamination problem. First, a slow but steady decrease in the measured frequency can be observed in time. The maximum recorded decrease in frequency was about 5 % after 8 continuous hours of levitation of a silicone–CCl_4 drop in distilled water. This slow change could be attributed to both a gradual modification of the properties of the drop interface and to the small temperature rise (approx. 0·5 °C per hour) in the levitation cell. The second observed phenomenon is a small scatter in measured resonance frequency for different drops of the same liquid and size (the volume of the drop can be controlled reliably within $\pm$ 0·2 % with a calibrated screw syringe). The maximum amplitude of such a scatter may reach 2 % for the same batch of prepared drop liquid and the same host sample. This will be the important limiting factor when the accuracy of this method is assessed.

Size dependence of f_2. Figure 4 is a logarithmic plot of the measured frequency squared f_2^2 as a function of the cube of the drop radius R^3 for a phenetole drop (1·22 cSt) in a mixture of water and methanol. A linear least-square fit procedure yields the power law

$$f_2 \propto R^{-1.51}.$$

This result is very close to Lamb's theoretical formula, which yields $f_2 \propto R^{-1.50}$.

As indicated above, the experimental uncertainty has been assessed to be less than $\pm$ 2 %. This figure is the maximum scatter obtained through measurements on several (approx. 5) drops of the same radius, and reflects the combined effects of contaminants, temperature change, drop-volume inaccuracy, and experimental error.

The period at resonance, determined by measurements on the oscilloscope trace during steady-state driven oscillations, was also compared to that measured during free decay. Within the measurement error ($\pm$ 1 %) the two periods were the same when the drive frequency was that yielding a $+90°$ phase shift for the drop response with

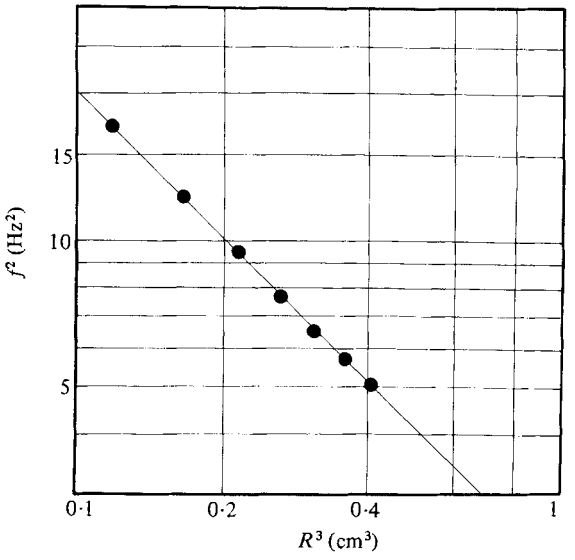

FIGURE 4. Data for phenetole drops (density approx. 0·96 g/cm^3) in distilled-water/methanol mixture. The square of the fundamental resonance frequency is plotted versus the cube of the drop radius on a logarithmic scale. The kinematic viscosity of phenetole is about 1·22 cSt, and the approximate interfacial tension is 16·5 dyn/cm.

respect to the drive. The resonance frequency determined at steady state was thus approximately the same as that of a freely decaying drop.

Figure 5 displays similar logarithmic plots for a series of mixtures of silicone oil with CCl_4 of various viscosities. The drops were suspended in distilled water. A least-square fit also yields coefficients very close to $-1{\cdot}5$. The various viscosity grades of the mixtures used had slightly different interfacial tensions, and consequently it was not possible to study the effects of viscosity upon the resonance frequency.

All the above measurements have been obtained with a 22 kHz standing wave used for levitation, and a modulated 66 kHz wave for the oscillation drive. It has been found that for small amplitude the results were, within experimental uncertainty, independent of the nature of the acoustic field.

Dependence on static distortion. An inspection of the static equilibrium shape of the levitated drop also revealed that the distortion due to buoyancy and radiation pressure forces (both static and time varying) was under 1 % from perfect sphericity for all the measurements reported here. *We shall therefore assume that the effects of such small non-sphericity are negligible.*

We have, however, also investigated the effects of more substantial distortions upon both the resonance frequency and the damping constant. This can be done by adding a static levitating standing wave to the time-modulated field, and by increasing its intensity. Both static oblate and prolate distortions may be obtained by using the appropriate frequency. They have been shown to have similar effects.

Even for small-amplitude oscillations, the resonance frequencies for the fundamental and first higher modes have been found to increase with distortion. Figure 6 displays the results for a 1·0 cm^3 phenetole drop and a 1·5 cm^3 silicone–CCl_4 mixture drop. Both drops have been statically deformed into the oblate spheroid shape. The

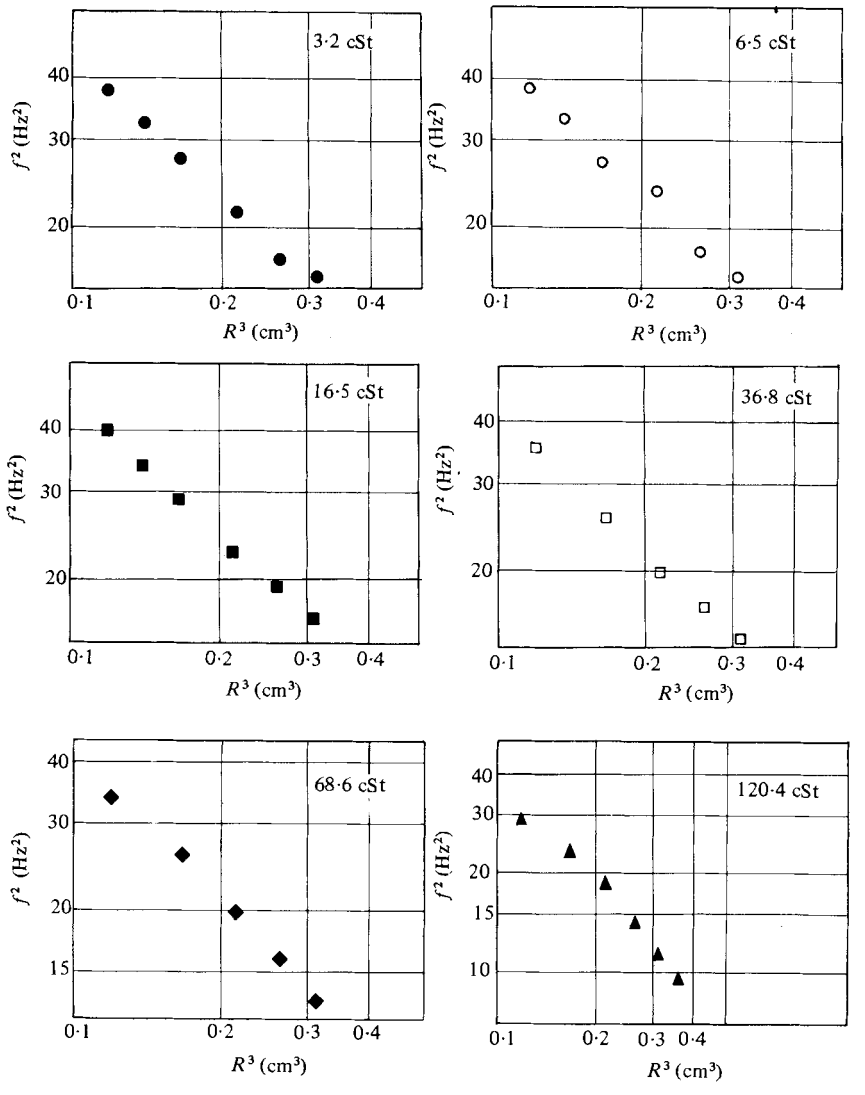

FIGURE 5. Experimental results for fundamental frequencies of drops of silicone/CCl_4 mixtures of various viscosities immersed in distilled water (density approx. 0·99 g/cm^3, interfacial tension between 35 and 40 dyn/cm). f^2 is plotted as a function of R^3. The kinematic viscosity ranges between 3·2 and 120·4 cSt. Drop radii range between 0·49 and 0·68 cm.

phenetole drop is driven into oscillation by a periodic compression at the poles, while the silicone–CCl_4 drop is driven by a periodic elongation at the poles. The distortion is characterized by the ratio of the long axis of the drop to the short axis (W/H). The percentage distortion is plotted on the horizontal axis, and the percentage increase in the fundamental resonance frequency f_2 on the vertical axis. An approximately linear variation of $\Delta f_2/f_2$ with increasing distortion is observed for both drops. In view of these results, a direct determination of the interfacial tension from acoustically measured resonance frequencies might not be as straightforward as it first appears.

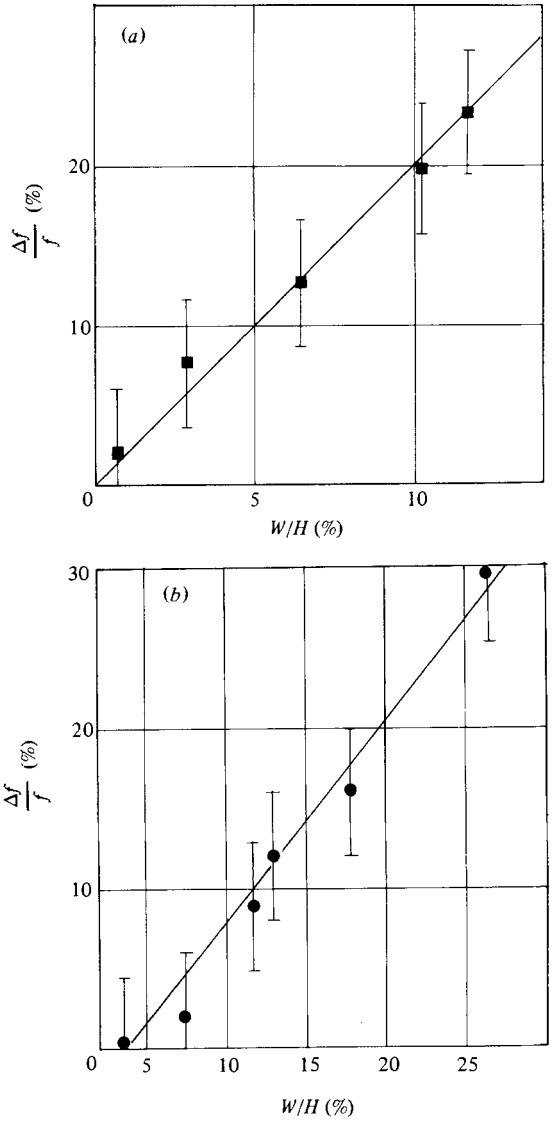

FIGURE 6. Variations of the fundamental resonance frequency with oblate deformation. The drops are statically deformed by the acoustic field. The resonance frequency is measured for small-amplitude oscillations. (*a*) Silicone/CCl_4, 1·5 cm^3 drop; (*b*) Phenetole, 1 cm^3 drop.

Higher-order modes ($L = 3, 4, 5$; $m = 0$)

The higher-order resonance modes are increasingly more damped than the fundamental, thus comparatively larger forces (i.e. acoustic pressures) are required to excite them. Under these conditions the static deformations of the drops are much more pronounced than during the fundamental-mode excitation. The measured frequencies will not then be those corresponding to a nearly spherical equilibrium shape as in the case discussed above.

Table 1 lists in columns 1–4 experimental values for the frequency of the modes corresponding to $L = 2$–5, for drops of both phenetole and silicone–CCl_4. The ratios

	f_2 (Hz)	f_3 (Hz)	f_4 (Hz)	f_5 (Hz)	$\frac{f_3}{f_2}$	$\frac{f_4}{f_2}$	$\frac{f_5}{f_2}$
Silicone/CCl_4 in water; 3·2 cSt, 1·9 cm^3							
Experimental	3·56 (± 0·07)	6·49 (± 0·13)	9·37 (± 0·19)	13·1 (± 0·25)	1·82 (± 0·07)	2·63 (± 0·1)	3·67 (± 0·15)
Lamb's formula					1·89	2·89	3·99
Theory (Marston 1980)					1·82	2·64	3·69
Silicone/CCl_4 in water; 3·2 cSt, 1·7 cm^3							
Experimental	3·66	6·81	10·21	13·65	1·86	2·79	3·73
Theory					1·86	2·79	3·74
Silicone/CCl_4 in water; 3·2 cSt, 1·5 cm^3							
Experimental	3·87	7·21	10·45	—	1·86	2·70	—
Theory					1·86	2·81	—
Phenetole in water/ methanol; 1·2 cSt, 1·5 cm^3							
Experimental	2·97	5·54	7·85	10·47	1·87	2·65	3·52
Theory					1·85	2·90	3·65

TABLE 1

f_L/f_2 are listed in columns 5–7. The theoretical predictions are listed under the experimental values in columns 5–7.

Figure 7 shows photographs of drops oscillating in the axisymmetric modes $L = 2$–4 ($m = 0$). The oscillation amplitudes shown here are quite appreciable and cannot be viewed as being small.

Swept frequency response

In order to obtain the true resonance curve of a drop, a very slow sweep through the frequency spectrum is required. For a 2·0 cm^3 drop a sweep rate of 10 mHz/s was adequate for the fundamental mode: the resonance curve obtained by such a sweep agrees with that obtained through a series of discrete steady-state measurements.

Figure 8 reproduces the experimental resonance curve for the fundamental mode for a 1·5 cm^3 silicone–CCl_4 drop in water. The shape of the curve for the fundamental mode is not quite symmetrical, and is characteristic of the response of a damped oscillator. For the case of a linear, damped harmonic oscillator, the resonance curve for the displacement has its maximum shifted to lower frequency with respect to the 'natural' frequency because of the damping term. The Q value of the fundamental resonant mode shown here is about 13 ($Q = f_2/\Delta f$, where Δf is the width of the resonance curve).

Figure 9 reproduces the mode spectrum of a 1·9 cm^3 silicone–CCl_4 drop in water. The various modes of oscillations are relatively well separated, and no unexpected resonance peak is found. This resonance-mode distribution is modified when larger-amplitude oscillations are studied. No quantitative information can be obtained from the relative heights of the various resonance peaks because the coupling of the radiation pressure forces to the liquid drop is not necessarily the same for different oscillation modes.

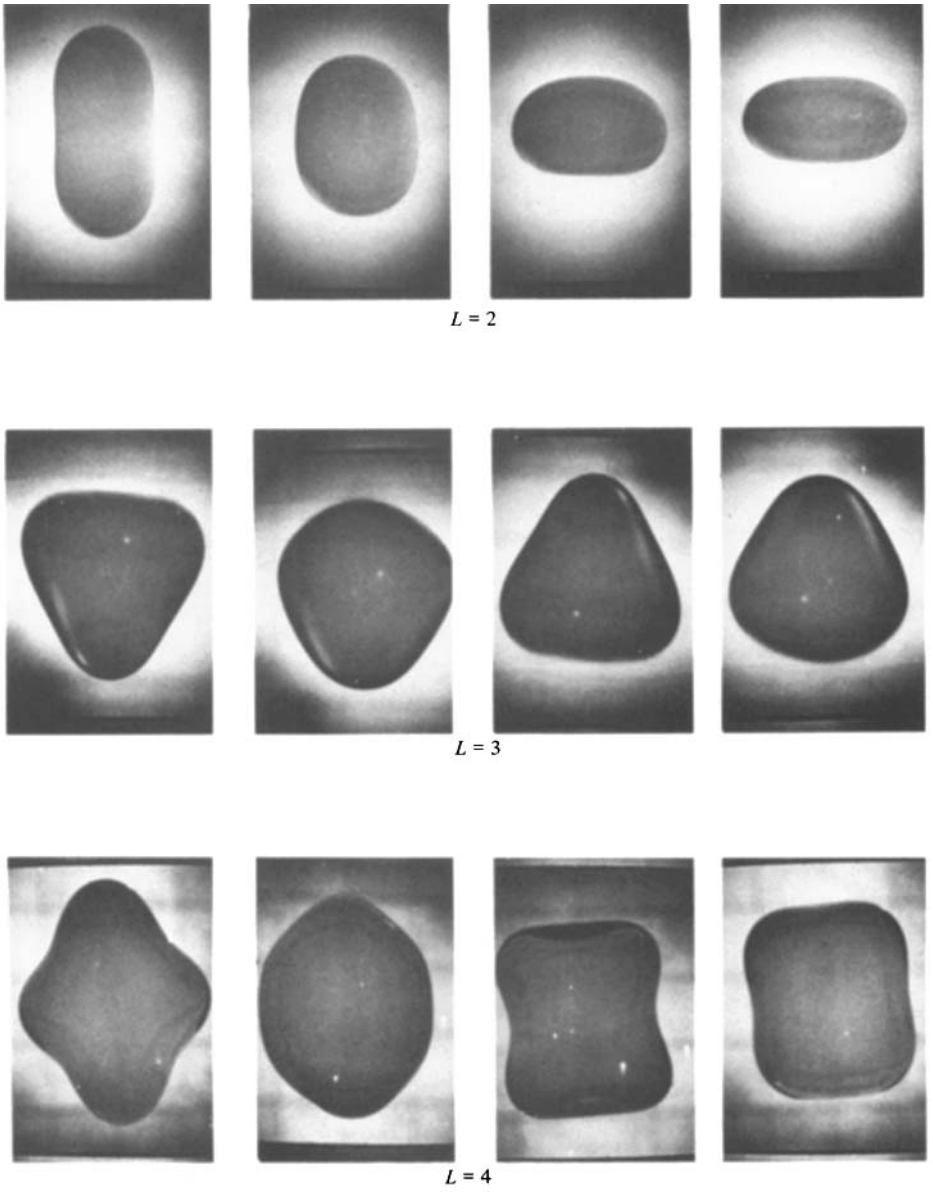

FIGURE 7. Photographs of drops oscillating in the $L = 2, 3, 4$ axisymmetric ($m = 0$) modes. The amplitudes of the oscillations shown here are much larger than those studied in this paper. They are shown here for the purpose of illustrating the various shapes.

5. Damping-constant measurements

The damping constant for the fundamental mode has been measured as a function of drop size, and of the viscosities of the inner and outer liquids. For viscosities lower than 100 cSt and drop volumes larger than 0·5 cm^3, data were obtained from photographs of oscilloscope traces taken during free decay. The experimental uncertainty was estimated to be around $\pm 5\,\%$. Determination of the Q value of the resonance

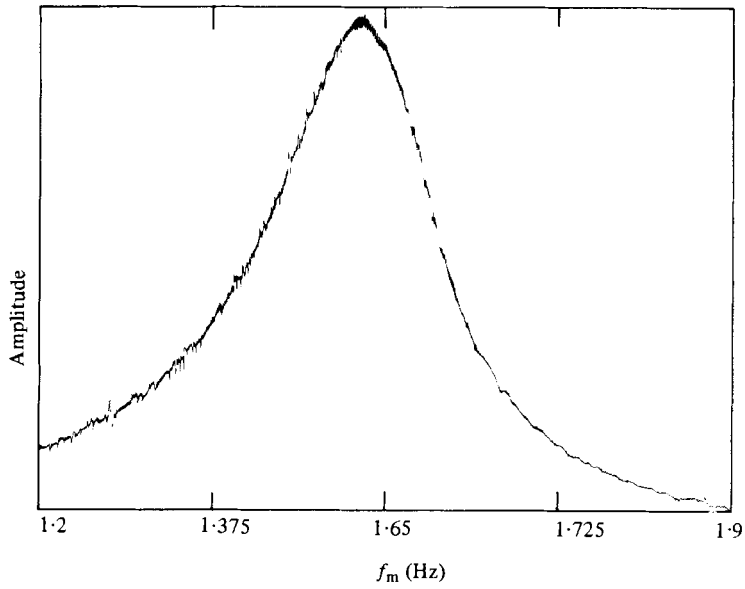

FIGURE 8. Swept frequency response of a 1·5 cm³ silicone/CCl_4 drop (3·2 cSt) immersed in distilled water. The resonance curve is for fundamental $L = 2$ mode.

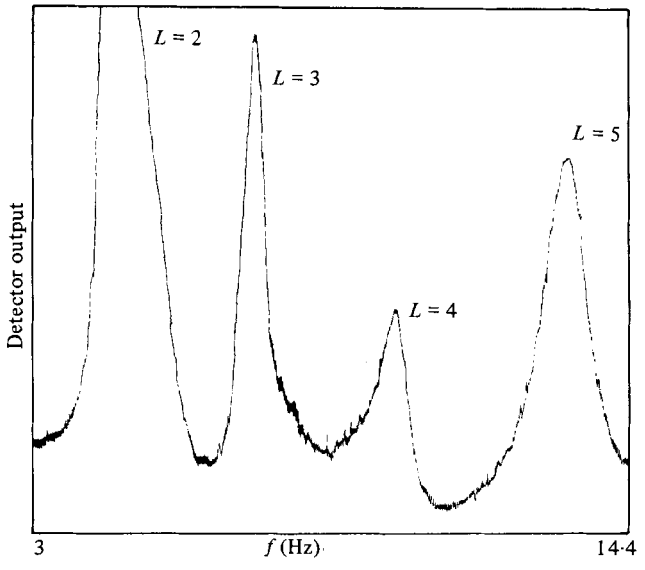

FIGURE 9. Resonant-mode spectrum of a 1·9 cm³ silicone/CCl_4 drop.

yielded damping-constant results which were generally about 10 % lower than the free decay data. Steady-state measurements through the frequency–phase relationship were characterized by a substantial scatter (15–20 %) of the results, although the average values were still within ± 10 % of the free-decay data. Of the three available methods, the one involving free-decay traces has been judged the most reliable and consistent. This is the method with which the bulk of the experimental data was taken. Figure 10 displays the photographs of a few decay curves for various viscosities.

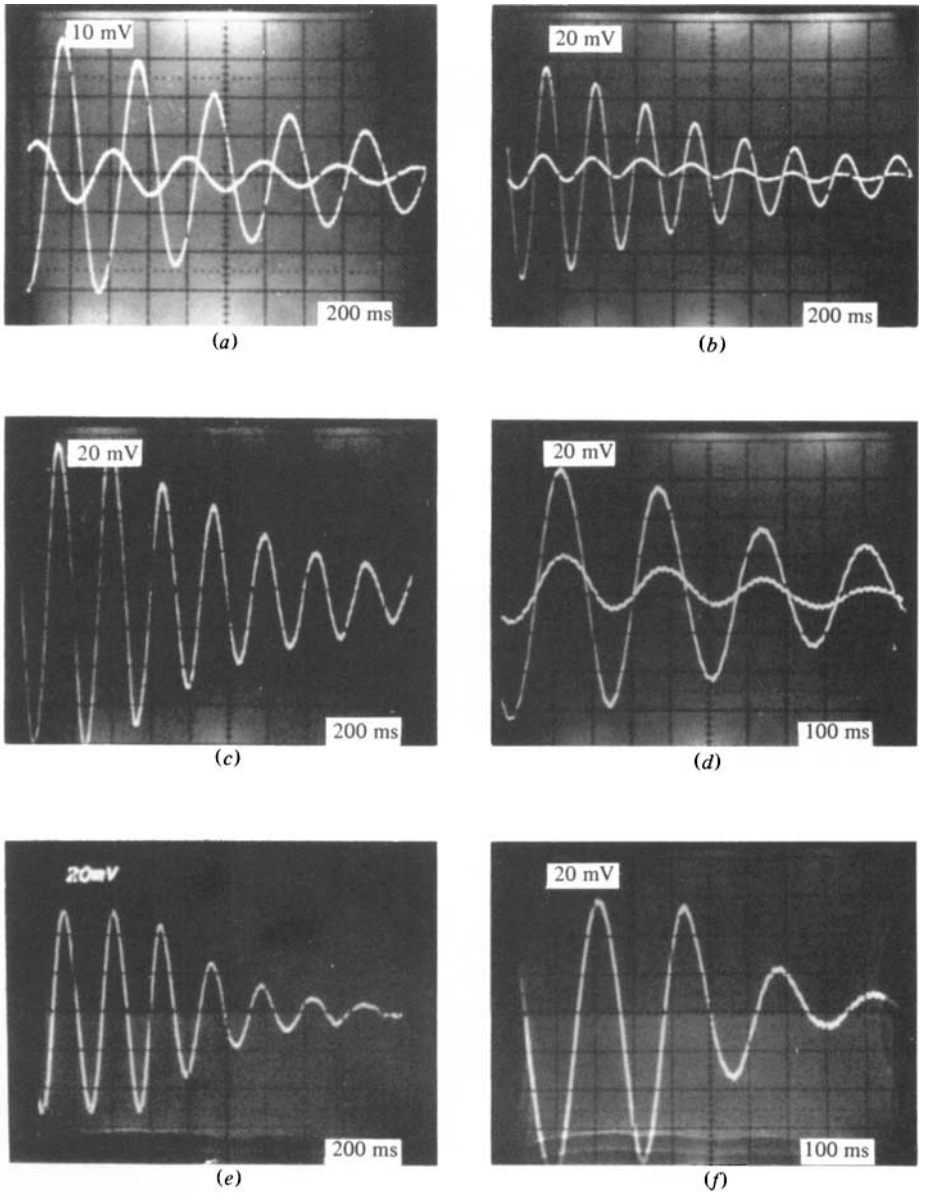

FIGURE 10. Photographs of oscilloscope decay traces for drops of various viscosities. Phenetole: (*a*) 1·22 cSt. Silicone: (*b*) 3·24 cSt; (*c*) 6·48 cSt; (*d*) 16·51 cSt; (*e*) 36·78 cSt; (*f*) 68·65 cSt.

The experimental results on the damping constant for phenetole (1·22 cSt), and for a series of mixtures of silicone oil and CCl_4 are given as functions of the drop radius in figure 11 *a*. Phenetole is characterized by the set of data with the lowest values. The increasing values of τ_2^{-1} are those for mixtures with kinematic viscosity equal to 3·25, 6·5, 16·5, 68·6 and 120·4 cSt, in this order.

A linear least-square fit of the phenetole data yields a power law

$$\tau_2^{-1} \propto R^{-1\cdot4}.$$

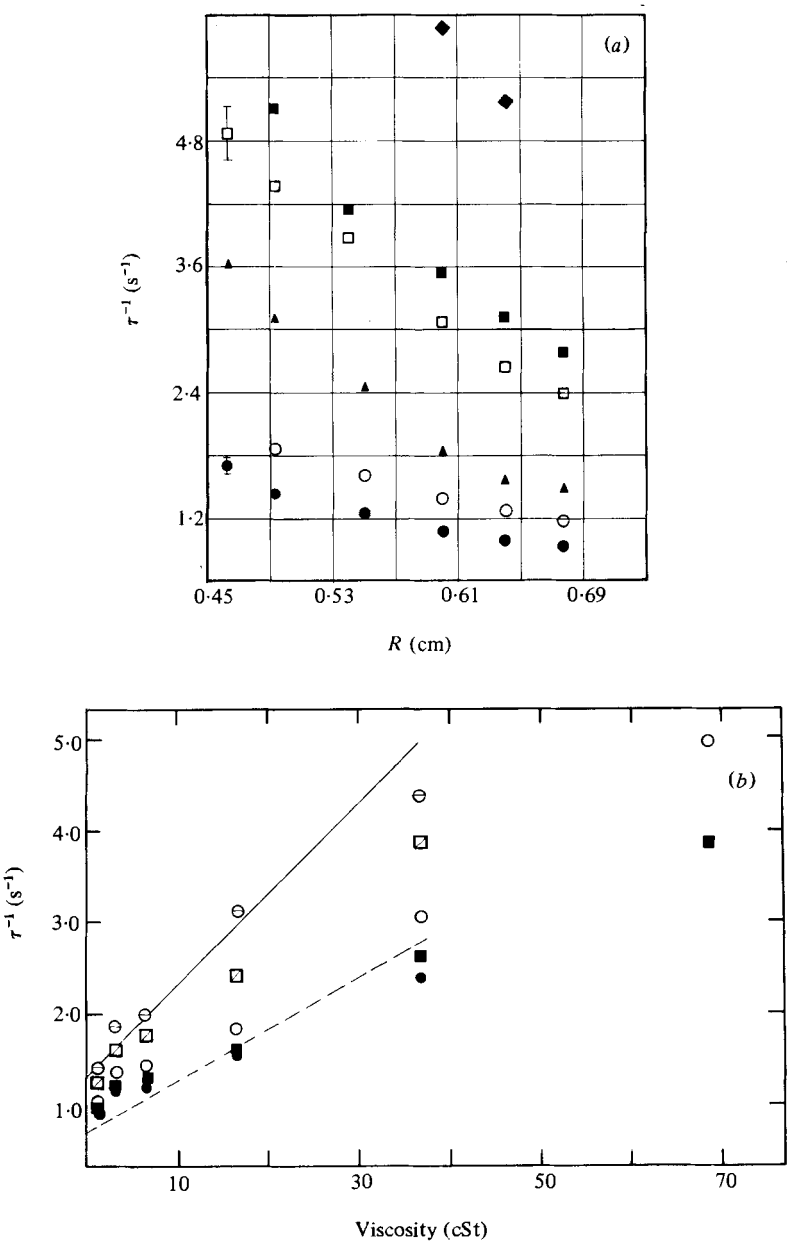

FIGURE 11. (*a*) Damping constant for various viscosity grades as a function of drop radius. ●, 1·2; ○, 3·2 cSt; ▲, 6·5 cSt; □, 16·5 cSt; ■, 36·8 cSt; ◆, 68·6 cSt. (*b*) Damping constant for various sizes as a function of kinematic viscosity. ●, 1·3 cm^3; ■, 1·1 cm^3; ○, 0·9 cm^3; ⊠, 0·7 cm^3; ⊖, 0·5 cm^3.

Although similar least-square fits of the data have been attempted for all the other liquids, the correlation obtained was not good. The resulting coefficients were also characterized by a substantial scatter. In addition to the inherent uncertainty, this scatter might indicate that the radius dependence of τ_2^{-1} is not really well represented by a simple power law of the type R^{-x}.

Volume (cm^3)	0·5	0·7	0·9	1·1	1·3	1·5
	Damping constant (s^{-1})					
Phenetole (1·22 cSt)						
Experiment	1·43	1·26	1·06	0·98	0·93	—
Theory (Marston 1980)	1·28	1·05	0·90	0·80	0·73	—
Silicone/CCl_4 (3·2 cSt)						
Experiment	2·09	1·61	1·38	1·28	1·16	0·94
Theory	1·54	1·27	1·09	0·96	0·89	0·75
Silicone/CCl_4 (6·5 cSt)						
Experiment	1·99	1·76	1·44	1·32	1·19	—
Theory	1·90	1·55	1·34	1·18	1·07	—
Silicone/CCl_4 (16·5 cSt)						
Experiment	3·13	2·43	1·83	1·58	1·46	—
Theory	2·95	2·40	2·08	1·82	1·65	—
Silicone/CCl_4 (36·8 cSt)						
Experiment	4·40	3·87	3·06	2·63	2·39	—
Theory	5·12	4·14	3·52	3·10	2·79	—
Silicone/CCl_4 (68·6 cSt)						
Experiment	—	—	4·97	3·88	—	—
Theory	—	—	5·88	5·16	—	—

TABLE 2

Figure 11*b* is a plot of the same experimental values as a function of viscosity for the various drop sizes. The host liquids used in these results are a water–methanol mixture ($\nu \simeq 1{\cdot}8$ cSt) for phenetole, and distilled water (approx. 1·1 cSt) for the silicone–CCl_4 drops. Table 2 lists the experimental values together with theoretical predictions for comparison purposes. The theoretical damping constants have been calculated under the assumption that the expression (1) for the resonance frequency is accurate.

One might also note that, as in the case of the resonance frequency, the damping coefficient appears to depend on the duration of suspension of the drop. A fast increase in τ_2^{-1} with time takes place initially, and then gives way to a slower increase. This might be attributable to a change in the interfacial properties of the liquids.

6. Internal fluid-particle flow

The motion of the drop-fluid particles during oscillation was described by Lamb in the case of small-amplitude slow vibrations in the fundamental mode. His predictions are found to agree with the outcome of our qualitative photographic study of internal flow.

The motion of the fluid inside the drop can be made visible by the addition of quasi-neutrally buoyant tracer particles. These markers should be small enough to follow the fluid motion, but large enough to scatter sufficient light for detection. In this work, we have used organic-dye particles in the silicone–CCl_4 mixtures. An excess amount of dye particles will remain suspended in the drop for a reasonably long time (over a few hours). The drop is illuminated by a thin sheet of light, and the 90° scattering is photographed with high-speed film. Depending upon the intensity of the scattered

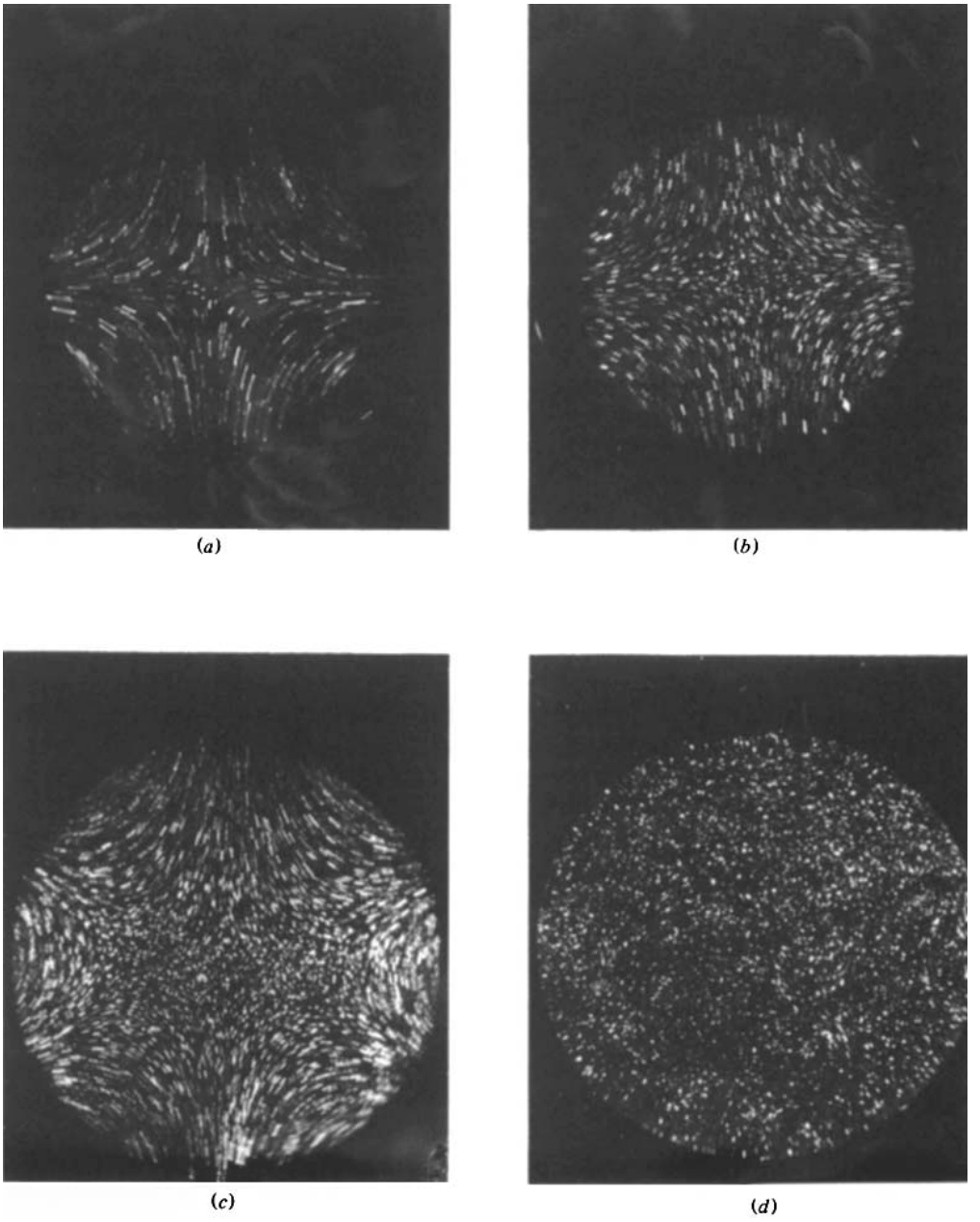

FIGURE 12. Flow patterns of suspended dye particles in drops oscillating in the $L = 2$ and $L = 3$ modes. (d) shows the dye particles inside a stationary drop.

light, the exposure time can be reduced to 0·5 s with 3000 ASA films and an $f/2{\cdot}5$ lens. Even-shorter exposure times may be obtained with faster lenses and films, or with a more intense illumination.

A detailed analysis of the particle motion in the transient stages is in the planning phase. At the present time we are only concerned with steady-state configurations. In addition, an accurate analysis of the particle flow field requires a correction for the

distortion caused by the curved surface of the drop and the difference in index of refraction between the two liquids. At the present time, however, we are restricting ourselves to a qualitative discussion.

Figure 12 shows photographs taken during steady-state driven oscillations in the $L = 2, m = 0$ and $L = 3, m = 0$ modes, as well as in the stationary state. The exposure times are all 2 s. For the $L = 2$ mode this corresponds to about the time for 5 complete oscillations, while the drop undergoes about 9 complete oscillations for the $L = 3$ mode. Only particles within a very thin slice at the mid-plane of the drop are illuminated.

Longer-time-exposure photographs (up to 5 min) of stationary drops have not revealed any steady motion within a levitated drop at equilibrium. This would suggest that gravity, acoustic forces, and streaming in the outside liquid do not cause any significant steady flow when the acoustic pressure remains low. A study of the internal flows resulting from acoustically distorted drops will be reported in a future communication.

By inspection of figure 12, one can find a region of almost stationary particles near the centre of the drop, both for the fundamental as well as for the first higher mode. The fluid particles found there before oscillation will be likely to remain there indefinitely if no other flow is induced. This might bear some relation to the centring force observed when a second drop of immiscible liquid is placed inside the first oscillating drop.

For the fundamental ($L = 2$) mode, the particle trajectories line up along hyperbolas in the four quadrants as predicted by Lamb. A fourfold symmetry is observed, and the particle paths appear linear. The displacement amplitude increases with radial distance from the drop centre, and the maximum excursions are found at the boundaries along the vertical and horizontal symmetry axes. Because of the axisymmetric nature of these particular oscillations and the requirements of volume conservation and incompressibility, the displacement amplitude is larger in the vertical-axis direction.

One should remark that these simple flow patterns are not retained when the oscillations grow to large amplitude. Our nonlinear study has revealed that a steady displacement of the particle trajectories is superimposed on this flow pattern.

The drop-shape oscillations will induce vibration of the particles in the outside liquid found in a boundary layer. From similar photographic observations the thickness of such a layer has been estimated to be as large as 30 % of the drop radius for a drop of approx. 1 cm diameter, and a frequency of approx. 4 Hz. A significant amount of energy is thus transferred to the outside fluid, and quite obviously this will result in a major contribution to the dissipation as derived from the theory.

7. Data interpretation and discussion

Resonance frequency

The radius dependence of f_2 has been found to be very close to Lamb's power law $R^{-1.5}$. This is in general agreement with the theory, which predicts only deviations less than 5 % from the values calculated from Lamb's formula. This particular point has not been checked, however, for a rigorous comparison would require a knowledge of the interfacial tension. This information is not available at the present time because the standard measurement techniques for that parameter do not yield reliable in-

formation when the density difference between the two liquids of interest is small (less than 1 % in this case). Under these circumstances, only a comparison between the experimental ratios f_L/f_2 of the resonance frequencies of the higher modes over the fundamental frequency and the theoretical predictions can be attempted. The results of such a comparison must be considered with caution, however, for the static shapes of the drops are not exactly the same when driving the fundamental and when exciting the higher modes, as we discussed above. It has been observed that the resonance frequency of a statically distorted drop (either in the prolate- or oblate-spheroid shape) is always higher than that of a spherical drop. Thus, if we denote by f_2' and f_3' those for a distorted drop, we would have the relationship

$$\frac{f_3'}{f_2} > \frac{f_3}{f_2}.$$

The experimental values (obtained for a non-spherical drop) would be higher than the true value of this frequency ratio. This discrepancy would presumably grow larger for higher-order resonance modes.

Inspection of table 1 reveals that the theoretical values for the frequency ratios are in good agreement with the experimental data. Lamb's predictions are about 4 % too large for f_3/f_2 and 8 % too large for f_5/f_2. The experimental uncertainty has been estimated to be less than 4 %. Hence, even accounting for the present uncertainty margin, the theoretical treatment appears to provide a closer agreement than Lamb's formula.

One might also wonder about the extent to which the static component of the acoustic radiation-pressure force influences the dynamics of the motion. A systematic error in the resonance frequency may arise because of the additional restoring component from the acoustic field. The ratio of the interfacial force to the static acoustic force may provide an approximate value for the resulting frequency increase. The interfacial force F_σ may be roughly evaluated as $2\sigma\pi R \simeq 150$ dyn for a 1 cm^3 drop of silicone–CCl_4 in water. The static acoustic force F_A is estimated to be at most 5 dyn. Thus, $F_\sigma/F_A \simeq 30$, or acoustic force is approximately 3·3 % of the interfacial tension force. The subsequent change in resonance frequency should then be about + 1·8 %. This is roughly the amount by which the acoustic measurements would overestimate the true resonance frequency according to the above simple reasoning.

Damping constant

Size dependence. From the experimental data, no simple function of the radius could be extracted, as had been possible with the resonance frequency. This is consistent with the theoretical claim that damping is significantly influenced by dissipation in the boundary layer around the drop. From table 2 one can observe that the radius dependence of τ_2^{-1} for the various liquids of different viscosity appears to be in rough agreement with theoretical predictions, although the magnitudes are often significantly different. The discrepancy between the experimental and theoretical values for τ_2^{-1} ranges between 5 and 30 % for the lower-viscosity grades. This is quite reasonable in view of the fact that contamination of the interface could not be avoided.

Viscosity dependence. The straight lines of figure 11(*b*) are plots of calculated damping constants derived from (1)–(5). Linear least-square fits of the data tend to yield a general agreement with this linear behaviour, although the experimental

Inside viscosity	Outside viscosity	Damping constant (s^{-1})
1·05 cSt		
Experiment	10 cSt	1·52 (± 0·1)
Theory (Marston 1980)		1·16
1·05 cSt		
Experiment	20 cSt	2·93 (± 0·15)
Theory		3·66
16·5 cSt		
Experiment	1·1 cSt	1·58 (± 0·1)
Theory		1·82
36·8 cSt		
Experiment	1·1 cSt	2·63 (± 0·15)
Theory		3·1

TABLE 3

constants of proportionality are different from the calculated ones. The rates of increase of τ^{-1} found experimentally are smaller than those derived theoretically. This tends to be more prominent for larger drops.

An interesting characteristic of these results may be found in the relationship between the experimental and calculated τ^{-1} as viscosity increases: for low viscosities the measured damping rates are higher than the results of calculations, but this relationship is reversed for the higher viscosities. It thus appears that the present theoretical treatments are more valid at low viscosity, or perhaps for the cases where outer and inner liquids have comparable viscosities. The physical origin of such a phenomenon might also be attributed to the inertia of the boundary layer. The damping measurements were performed by abruptly shutting off the drive during steady-state oscillation. Presumably, the flow field just before the drive cut-off would be well-established with the fluid in the boundary layer oscillating with the drop boundaries. The damping mechanism of the drop must be influenced by the inertia of the moving fluid in the boundary layer. In this case, because the motion in the outer liquid is not damped as quickly as in the more viscous drop, there might be a residual drive supplied by the boundary-layer motion, thereby slightly decreasing the damping rate.

Damping measurements have also been performed with different outer liquid viscosities. Table 3 summarizes the results. 10 and 20 cSt mixtures of water and glycerine were used as host liquids for 1·1 cm^3 drops of phenetole. The resulting increase in damping rate is larger than if the inside viscosity was raised by the same amount and the outside viscosity unchanged. This indicates that for the present drop size the influence of the outer fluid viscosity is more substantial than that of the inner fluid.

An uncertainty is introduced by the time variation of the surface properties of the immersed drops. It was observed, however, that a state of slow change was always attained after levitation over about 30 minutes. The scatter was reduced significantly after precautions had been taken to perform measurements during that stage. Another source of error affecting the accuracy of absolute measurements arises from the changes in properties of liquids used on different days. In order to overcome this difficulty, the radius-dependence measurements were always made for a series of drops from the same batch of mixture and with the same host. The viscosity dependence of the

damping constant is more seriously affected by this drawback, and the results should be slightly more uncertain.

Dependence of the decay rate on the levitation force. The decay rate has also been found to increase when the intensity of a static levitating acoustic field is increased. With a 4 % distortion in the oblate shape, a 13 % rise in the damping constant has been obtained. Such a large increase cannot be explained by the higher resonance frequency alone, as suggested by the theoretical results (equation (4)). No explanation of such a phenomenon can be provided at the present time, but it strongly suggests that the dissipation rate of drop-shape oscillations is quite sensitive to the influences of external forces.

8. Summary and conclusion

Driven shape oscillations of liquid drops under reasonably well-controlled conditions have allowed the determination of the resonance frequencies of the first few modes. The configurations of the oscillating drops resemble closely those predicted. The time dependence of the oscillation amplitude is very close to sinusoidal for free vibrations, but the time spent in the various configurations characteristic of each mode depends strongly on the acoustic drive for driven oscillations. For example, in the case of the fundamental axisymmetric mode, a freely oscillating drop spends only a very slightly longer time in the prolate configuration, while a driven drop might be found in the prolate shape during a longer, equal, or shorter time, depending upon the driving mode.

For small-amplitude oscillations, a drop suspended in a host liquid behaves in a way very similar to the usual damped harmonic linear oscillator in many respects: the response to a sinusoidal excitation is almost purely sinusoidal, the frequency of maximum response is characterized by an approximately 90° phase shift between the drive and the response, the decay rate is roughly linear with the drop viscosity, and the resonance curve for the displacement has the familiar shape.

An important difference arises from the presence of the outer support liquid which not only adds additional inertia, but also plays an important role in the dissipation mechanism, as predicted by the theory (Marston 1980). For low viscosity (less than 20 cSt), and drop volumes between 0·5 and 2 cm^3 the dissipation mechanism is dominated by the energy loss through the boundary layer at the drop surface. As the viscosity of the inner fluid grows larger, however, the theoretical predictions appear to overestimate the dissipation rate. This has been tentatively attributed to the residual momentum of the boundary-layer fluid. Study of the internal fluid particle flow has revealed a quasi-potential flow field with no noticeable circulation, thereby confirming Lamb's predictions and the validity of the theoretical assumptions.

The acoustical-levitation technique allows a non-invasive experimental study of the dynamics of oscillating drops if some precautions are taken to minimize the influence of the acoustic fields. A detailed quantitative analysis is needed in order to determine exactly the extent of the influence of acoustic forces, but it is reasonable to assume that, for very small levitating forces and oscillation amplitudes, their disturbing effect upon the dynamics of the drop vibrations is quite small.

This work was carried out at the Jet Propulsion Laboratory under Contract No. NAS 7-100, sponsored by the National Aeronautics and Space Administration.

REFERENCES

JACOBI, N., TAGG, R., KENDALL, J., ELLEMAN, D. & WANG, T. 1979 Free oscillations of a large drop in space. *17th Aerospace Sciences Meeting*, paper 79-225.

LAMB, H. 1932 *Hydrodynamics*, pp. 473–639. Cambridge University Press.

MARSTON, P. 1980 *J. Acoust. Soc. Am.* **67**, 15.

MARSTON, P. & APFEL, R. 1979 *J. Colloid Interface Sci.* **68**, 280.

MARSTON, P. & APFEL, R. 1980 *J. Acoust. Soc. Am.* **67**, 27.

MILLER, C. & SCRIVEN, L. 1968 *J. Fluid Mech.* **32**, 417.

PROSPERETTI, A. 1980*a* *J. Méc.* **19**, 149.

PROSPERETTI, A. 1980*b* *J. Fluid Mech.* **100**, 333.

TRINH, E. & WANG, T. 1980 A quantitative study of some non-linear aspects of drop shape oscillations. Paper presented at the 100th Meeting of the Acoustical Society of America.

WANG, T., SAFFREN, M. & ELLEMAN, D. D. 1974 Drop dynamics in space. In *Proc. Int. Colloquium on Drops and Bubbles*, p. 266.

WANG, T. 1979 *Proc. IEEE Ultrasonics Symp.*, pp. 471–475.

YOSIOKA, K. & KAWASIMA, Y. 1955 *Acustica* **5**, 167.